

Original article

# Age related signal changes of the pituitary stalk on thin-slice magnetic resonance imaging in infants

Takashi Okazaki <sup>a</sup>, Tetsu Niwa <sup>a,\*</sup>, Keiji Suzuki <sup>b</sup>, Shuhei Shibukawa <sup>c</sup>, Yutaka Imai <sup>a</sup>

<sup>a</sup> Department of Radiology, Tokai University School of Medicine, 143 Shimokasuya, Isehara 259-1193, Japan

<sup>b</sup> Department of Pediatrics, Tokai University School of Medicine, 143 Shimokasuya, Isehara 259-1193, Japan

<sup>c</sup> Department of Radiology, Tokai University Hospital, 143 Shimokasuya, Isehara 259-1193, Japan

Received 8 August 2018; received in revised form 24 October 2018; accepted 19 November 2018

## Abstract

**Purpose:** Signals of some brain regions change along with development in T1-weighted imaging (T1WI) in infants. This study aimed to assess the association of the signal intensity of the pituitary stalk on thin-slice T1WI with infant age.

**Methods:** This retrospective study was performed in 89 infants (gestational age [GA], 25–41 weeks; postmenstrual age [PMA], 36–46 weeks; chronological age [CA], 4–141 days) without intracranial abnormalities. The signal ratio of the pituitary stalk/pons on thin-slice T1WI was calculated, and its correlations with GA, PMA, and CA were assessed. Additionally, the signal ratio of the anterior pituitary gland/pons was calculated, and its correlation with that of the pituitary stalk was assessed. The signal intensity and distribution of the pituitary stalk were visually rated, and their correlations with GA, PMA, and CA were assessed.

**Results:** The signal ratio of the pituitary stalk was significantly positively correlated with GA ( $P < 0.001$ ) and negatively correlated with CA ( $P < 0.001$ ), but was not correlated with PMA. Stepwise multiple regression revealed that CA was independently associated with the signal ratio of the pituitary stalk ( $P < 0.001$ ). GA was significantly higher ( $P < 0.05$ ) and CA was significantly lower ( $P < 0.05$ ) in infants with a high signal intensity and wide distribution of high signal intensity of the pituitary stalk.

**Conclusions:** The signal intensity of the pituitary stalk on T1WI was negatively correlated with CA in infants, which might be related to postnatal changes in the pars tuberalis of the pituitary stalk after birth in infants.

© 2018 The Japanese Society of Child Neurology. Published by Elsevier B.V. All rights reserved.

**Keywords:** Infant; Pituitary stalk; Magnetic resonance imaging; T1-weighted imaging; Chronological age; Gestational age

## 1. Introduction

With the recent progress in magnetic resonance (MR) imaging, infants are increasingly undergoing MR imaging to assess neurodevelopment and brain injuries [1,2]. MR imaging findings should be accurately interpreted with knowledge about normal neuroimaging findings. However, this is sometimes difficult, as normal MR find-

ings change with development. MR imaging of an infant's brain shows signal changes associated with myelination. The progress of myelination is seen as relatively high signal intensity on T1-weighted imaging (T1WI), which reflects increases in lipids, predominantly galactocerebroside, and cholesterol, within the myelin membrane [3,4]. The progression pattern of myelination can be used to assess brain development. On T1WI, it is important not to assess myelination according to gestational age (GA) or chronological age (CA) but to assess it according to postmenstrual age (PMA: GA + CA) [5–

\* Corresponding author.

E-mail address: niwat@tokai-u.jp (T. Niwa).

7], particularly in preterm infants. However, some brain regions show high signal intensity on T1WI at birth and a subsequent signal decrease after birth. These regions include the anterior pituitary gland, subthalamic nucleus, globus pallidus, stria medullaris thalami, fornix, cerebellar vermis, and dentate nucleus [8–10]. Additionally, many lesions, such as ischemic, metabolic, and infectious lesions and lesions related to neurocutaneous syndrome, tend to show a relatively high signal intensity on T1WI in infants with less advanced myelination [11,12]. Therefore, knowledge about normal MR imaging findings is crucial for the accurate interpretation of the infant brain.

Preterm infants are usually screened with MR imaging at term-equivalent age (TEA) [13], as there is a relatively high risk of brain injury. Additionally, near-term and term infants are screened for brain lesions when some clinical situations, such as hypoxia, hypoglycemia, and suspicion of infection or metabolic disease, are present. Although infants have a small head size, recent 3-T MR imaging provides a relatively high signal-to-noise ratio, enabling thin-slice imaging [14,15]. When using thin-slice MR imaging in clinical practice, we found that the pituitary stalk has various signal intensities on T1WI in infants. As the signal changes of the pituitary gland after birth are known [8], we hypothesized that the signal intensity of the pituitary stalk has some relation to infant age. Such knowledge is crucial for the accurate interpretation of development and further assessment of the infundibular regions in infants. The present study aimed to assess the association of the signal intensity of the pituitary stalk with infant age (GA, PMA, and CA) in order to clarify the characteristics of pituitary stalk findings.

## 2. Materials and methods

### 2.1. Subjects

This retrospective study was approved by our Institutional Review Board, and the requirement for informed consent was waived. In our institution, preterm infants were screened using MR imaging at TEA or near TEA. Term infants also underwent MR imaging when an intracranial insult was suspected. The timing for MR examination depended on the clinical reason (mean age for term infants at MR examination was 11.6 days). Between August 2013 and December 2016, 195 consecutive infants underwent MR imaging, including thin-slice T1WI of the brain. A total of 107 infants without any intracranial abnormalities were selected. However, 18 infants were excluded (motion artifacts, 11; incomplete MR examination without thin-slice T1WI, 4; history of cardiopulmonary arrest, 1; suspicion of tuberous sclerosis, 1; unknown gestational age, 1). Finally, 89 infants (45 boys and 44 girls; GA, 25–41 [mean, 32.4] weeks;

PMA, 36–46 [mean, 39.2] weeks; CA, 4–141 [mean 47.7] days) were included. The main purpose of MR examination in these infants was screening for premature delivery (70 infants), partial asphyxia (9 infants), an apneic event or suspicion of an apneic event (5 infants), jaundice (2 infants), hypoglycemia (1 infant), meconium aspiration syndrome (1 infant), and suspicion of fetal cerebellar abnormality (1 infant).

### 2.2. MR imaging

MR imaging was performed using 3-T clinical scanners (Achieva Tx or Ingenia, Philips, The Netherlands). An 8-channel head coil was used for the Achieva Tx system, and a 12-channel head coil was used for the Ingenia system. Routine MR sequences included axial T1-weighted spin-echo imaging, T2-weighted fast spin-echo imaging, diffusion-weighted imaging, sagittal thin-slice T1WI, and susceptibility-weighted imaging. Sagittal thin-slice T1WI was performed using a 3D gradient-echo sequence with the following parameters: repetition time/echo time, 9.5/4.4 ms; inversion time, 1200 ms; matrix,  $192 \times 174$ ; field of view,  $160 \times 143$  mm; flip angle,  $8^\circ$ ; slice thickness, 0.9 mm; average number, 1; slice number, 120; turbo factor (number of data samplings per shot), 200; parallel imaging sensitivity encoding factor, 1.5; and acquisition time, 2 min 52 s. The imaging resolution was  $0.83 \times 0.82 \times 0.90$  mm. Sedation agents were not used for MR scanning. Infants were wrapped with a vacuum pillow (VMR433X01, Rikutou, Tokyo, Japan) to reduce their movements during MR scanning.

### 2.3. Quantitative image analysis

Regions of interest (ROIs) were placed on thin-slice T1WI images. Signal intensity of the pons was used for normalization to evaluate that of the pituitary stalk in infants on the two MR scanners. A rectangular ROI was placed around the pituitary stalk, and a round ROI was placed at the anterior pituitary gland and basilar part of the pons (Fig. 1). All ROIs were placed by a single radiologist with 7 years of experience in pediatric neuroradiology (T.O.), using ImageJ software version 1.5 (National Institutes of Health). The signal ratios of signal intensities of the pituitary stalk (signal-ratio<sub>stalk</sub>) and anterior pituitary gland (signal-ratio<sub>ant</sub>) to that of the pons were calculated using the following formulas:

$$\text{Signal - ratio}_{\text{stalk}} = S_{\text{stalk}} / S_{\text{pons}}$$

$$\text{Signal - ratio}_{\text{ant}} = S_{\text{ant}} / S_{\text{pons}}$$

where  $S_{\text{stalk}}$ ,  $S_{\text{ant}}$ , and  $S_{\text{pons}}$  are the mean signal intensities of the pituitary stalk, anterior pituitary gland, and pons in the ROIs, respectively.

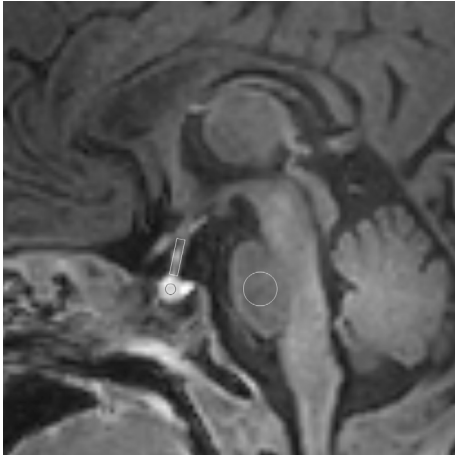


Fig. 1. Thin-slice T1-weighted imaging illustrates the region of interest (ROI) measurements. Square ROI at the periphery of the pituitary stalk and round ROIs at the anterior pituitary gland and pons.

#### 2.4. Qualitative image analysis

The signal intensity of the pituitary stalk on thin-slice T1WI was independently assessed by two radiologists with 17 and 7 years of experience in pediatric neuroradiology (T.N. and T.O., respectively) in random order. The readers were blinded to the GA, PMA, and CA of the infants. In the first session, the signal intensity of the pituitary stalk was compared to that of the pons and was rated by using the following scores: 0, prominently lower; 1, slightly lower; 2, iso-intense; 3, slightly higher; and 4, prominently higher. In the second session, the signal intensity of the pituitary stalk was compared to that of the anterior lobe of the pituitary gland and was rated according to the same scores mentioned above. In the third session, the distribution of high signal intensity in the pituitary stalk was assessed by two readers with consensus according to the following scores: 0, no high signal intensity; 1, spotted; 2, less than half of the pituitary stalk; 3, more than half of the pituitary stalk.

#### 2.5. Statistical analysis

All statistical data were analyzed using a software package (MedCalc, version 18.2.1; MedCalc Software bvba, Ostend, Belgium). To assess the relationship of the signal-ratio<sub>stalk</sub> with infant age, the signal-ratio<sub>stalk</sub> was compared to GA, PMA, and CA using Spearman correlation and a stepwise multiple regression analysis. The relationship of the signal intensities of the pituitary stalk and anterior pituitary gland was assessed according to the signal-ratio<sub>stalk</sub> and signal-ratio<sub>ant</sub> using Pearson correlation. The relationships of the scores of the pituitary stalk with GA, PMA, and CA were assessed using the Kruskal–Wallis test with post-hoc analysis.

Interobserver agreements were assessed using intraclass correlation coefficients (ICCs). ICCs were interpreted by using the following criteria reported by Landis and Koch [16]: 0.01–0.20, slight agreement; 0.21–0.40, fair agreement; 0.41–0.60, moderate agreement; 0.61–0.80, substantial agreement; and 0.81–1.0, near-perfect agreement. A  $P$ -value  $< 0.05$  was considered statistically significant.

### 3. Results

#### 3.1. Quantitative image analysis

The mean signal-ratio<sub>stalk</sub> was 1.06 (range, 0.70–1.64). The signal-ratio<sub>stalk</sub> was significantly positively correlated with GA (Spearman  $\rho = 0.52$ ,  $P < 0.001$ ) and negatively correlated with CA (Spearman  $\rho = -0.59$ ,  $P < 0.001$ ). Additionally, the signal-ratio<sub>stalk</sub> was negatively correlated with PMA; however, the Spearman  $\rho$  value was relatively low (Spearman  $\rho = -0.34$ ,  $P = 0.001$ ). Stepwise regression analysis revealed that CA was an independent factor associated with the signal-ratio<sub>stalk</sub> ( $P < 0.001$ , Fig. 2). The mean signal-ratio<sub>ant</sub> was 1.57 (range, 1.05–2.64). A positive correlation was found between the signal-ratio<sub>stalk</sub> and signal-ratio<sub>ant</sub> ( $r = 0.56$ ,  $P < 0.001$ ). All signal-ratio<sub>stalk</sub> values were lower than signal-ratio<sub>ant</sub> values (mean, 0.69 [range, 0.42–0.94] fold).

#### 3.2. Qualitative image analysis

The scores for the signal intensity of the pituitary stalk were 2–4 (median, 3.0) for reader 1 and 2–4 (median, 3.0) for reader 2. There were no infants with a score of 0 or 1 (both readers). According to these scores for the pituitary stalk, GA and CA were significantly different ( $P < 0.001$ ) for both readers. A post-hoc test showed that GA was significantly higher and CA was significantly lower in infants with a higher score for the pituitary stalk ( $P < 0.05$ , respectively) (Figs. 3 and 4, Table 1). On the other hand, PMA did not significantly differ among the infants with each score for the signal intensity of the pituitary stalk. Interobserver agreement for the scores of the pituitary stalk was substantial (ICC = 0.80).

Scores for the comparison of the signal of the pituitary stalk to that of the anterior pituitary gland were 1 in 13 infants (14.1%) and 2 in 76 infants (85.4%) for reader 1 and were 1 in 33 infants (37.1%) and 2 in 56 infants (62.9%) for reader 2. There were no infants with a score 0, 3, or 4 (both readers).

The scores for the distribution of high signal intensity in the pituitary stalk were 0 in 26 infants (29.2%), 1 in 35 (39.3%), 2 in 25 (28.1%), and 3 in 3 (3.4%). According to these scores for the signal distribution, GA and CA were significantly different ( $P < 0.001$ ) (Table 2). A post-hoc

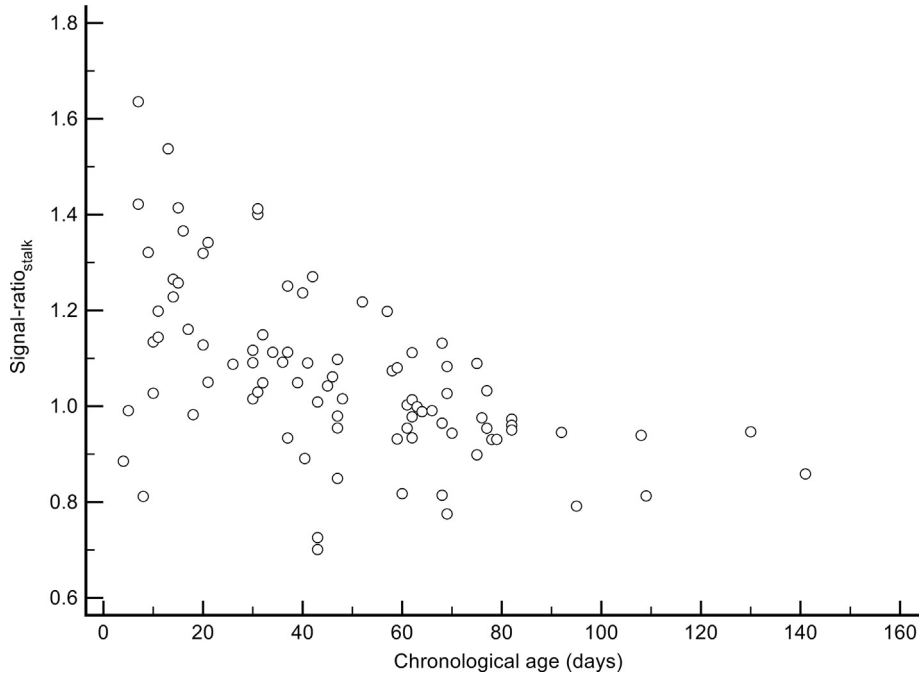


Fig. 2. Scatterplots show a significant negative correlation between the signal ratio of the pituitary stalk/pons ( $\text{signal-ratio}_{\text{stalk}}$ ) and chronological age (Spearman  $\rho = -0.59$ ,  $P < 0.001$ ).

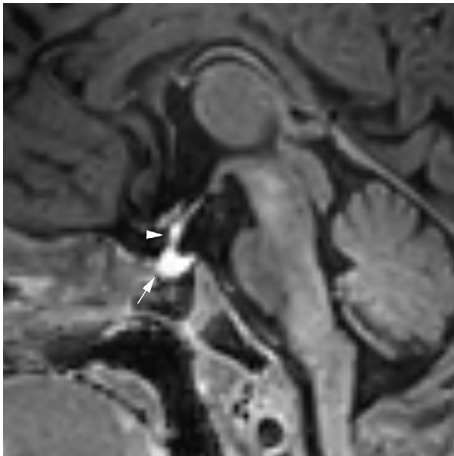


Fig. 3. Thin-slice T1-weighted imaging in a term infant (gestational age of 40 weeks and chronological age of 8 days) shows high signal intensity at both the pituitary stalk (arrowhead) and the anterior pituitary gland (arrow). Note that the high signal intensity is widely distributed in the pituitary stalk.

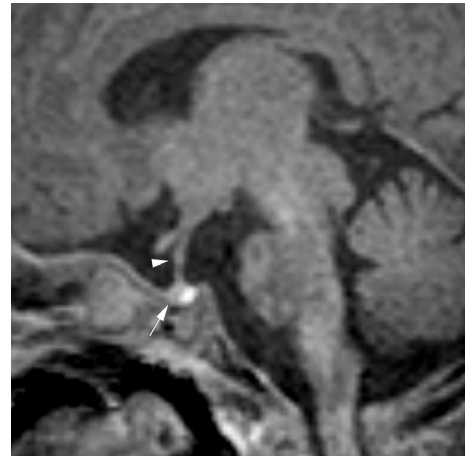


Fig. 4. Thin-slice T1-weighted imaging in a preterm infant (gestational age of 28 weeks, postmenstrual age of 40 weeks, and chronological age of 82 days) shows similar intensity at the pituitary stalk (arrowhead) and anterior pituitary gland (arrow) when considering the pons.

test showed that GA was significantly higher in infants with a higher score among those with scores of 0–2 ( $P < 0.05$ ) and that CA was significantly lower in infants with a higher score among those with scores of 0–2 ( $P < 0.05$ ) (Figs. 3–5).

#### 4. Discussion

We found that the signal intensity of the pituitary stalk varied on T1WI in infants. The intensity was pos-

itively correlated with GA and negatively correlated with CA. However, that was less likely to be correlated with PMA. These results suggest that the signal intensity of the pituitary stalk on T1WI decreases after birth in infants. Additionally, CA was independently correlated with the signal intensity of the pituitary stalk. Because brain development is usually considered for PMA, this knowledge is useful for correct interpretation of the infundibular region.

Anatomically, the pituitary stalk consists of a concentric zonal structure, including the central infundibular

Table 1  
Relationship between the scores for the signal intensity of the pituitary stalk and infant age.

Age	Score			P-value
	2	3	4	
<i>Gestational age (weeks)</i>				
Reader 1	29.1 (25.3–38.7)*	31.4 (25.4–40.3)*	35.9 (31.4–41.4)*	< 0.001
Reader 2	28.7 (25.3–36.3)*	31.4 (26.4–39.4)*	34.6 (31.4–41.4)*	< 0.001
<i>Postmenstrual age (weeks)</i>				
Reader 1	40.0 (37.1–46.1)	38.6 (36.6–44.0)	38.4 (36.4–43.9)	0.07
Reader 2	39.4 (37.1–46.1)	38.8 (36.6–46.0)	37.9 (36.4–42.9)	0.08
<i>Chronological age (days)</i>				
Reader 1	69 (10–141)*	47 (9–130)*	15 (4–41)*	< 0.001
Reader 2	69 (37–141)*	47 (4–108)*	16 (7–42)*	< 0.001

A greater score indicates more prominent high signal intensity of the pituitary stalk. There were no cases with a score of 0 or 1.

Data are presented as median with range in parenthesis.

\* Significant difference in post-hoc analysis ( $P < 0.05$ ) between each infant group according to the scores.

stem of the neurohypophysis and the peripheral pars tuberalis of the adenophysis [17,18]. In this study, a correlation was found between the signals of the pituitary stalk and anterior pituitary gland. Additionally, visual assessment showed that the signal intensity of the pituitary stalk was iso-intense or slightly lower when compared to that of the anterior pituitary gland. These results suggest that a high signal intensity in the pituitary stalk might be associated with factors similar to those in the anterior pituitary gland. The anterior pituitary gland usually appears with high signal intensity on T1WI at birth, and the intensity subsequently reduces after birth [8]. A high signal intensity on T1WI in the anterior pituitary gland in the neonatal period is explained to be associated with a high amount of endoplasmic reticulum and high protein synthetic activity by the increase in the number of prolactin cells after

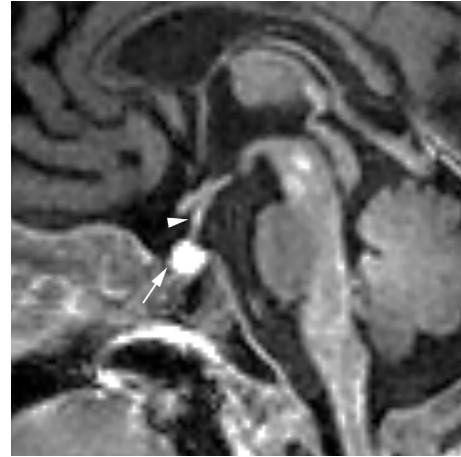


Fig. 5. Thin-slice T1-weighted imaging in a preterm infant (gestational age of 34 weeks, postmenstrual age of 37 weeks, and chronological age of 21 days) shows partial distribution of high signal intensity in less than half of the stalk (arrowhead). The anterior pituitary gland shows high signal intensity (arrow).

the 25th gestational week, which is induced by estrogen from the placenta during pregnancy [8,19,20]. The signal decrease in the anterior pituitary gland is suggested to be related to the postnatal reduction of estrogen, which is produced by the placenta during pregnancy [21,22]. Accordingly, we assume that high signal intensity on T1WI at the pituitary stalk reflects neonatal hyperactivity of the pars tuberalis, which is similar to that in the anterior pituitary gland.

Development of the pituitary gland and pars tuberalis has not been fully elucidated, but understanding that is based on the studies of mouse [23]. Therefore, the development of the pars tuberalis during the human preterm period is not well understood. However, a fetal cadaver study [24] demonstrated histologic presence of the pars tuberalis at 25–30 weeks of age. In addition, the perinatal activity of the pars tuberalis was reported in rats [25]. These facts also suggest hyperactivity of pars tuberalis in human perinatal period.

The distribution of high signal intensity of the pituitary stalk was smaller in infants with lower GA and

Table 2  
Relationship between the scores for the distribution of high signal intensity of the pituitary stalk and infant age.

Age	Score				P-value
	0	1	2	3	
Gestational age (weeks)	29.0 (25.0–38.0)*	31.0 (25.0–41.0)*	33.0 (29.0–40.0)*	34.0 (33.0–40.0)	<0.001
Postmenstrual age (weeks)	40.0 (37.1–46.1)	38.7 (36.6–44.0)	38.4 (36.7–43.9)	36.7 (36.4–41.6)	0.104
Chronological age (days)	69 (10–141)*	46 (5–130)*	31 (4–68)*	15 (8–20)	<0.001

A greater score indicates larger distribution of high signal intensity in the pituitary stalk.

Data are presented as median with range in parenthesis.

\* Significant difference in post-hoc analysis ( $P < 0.05$ ) between each infant group according to the scores.

higher CA, suggesting that not only the signal intensity but also the area of high signal intensity in the pituitary stalk reduces after birth. Although pars tuberalis locates periphery of the pituitary stalk continuing from the anterior pituitary gland, high signal intensity, if identified, was generally seen in a part of the stalk in most infants. However, the reason for this inhomogeneous signal distribution in the pituitary stalk is unclear. The signal intensity of the pituitary stalk was correlated with that of the anterior pituitary gland, but it was lower than that of the anterior pituitary gland. This partial distribution of high signal intensity in the pituitary stalk might be associated with signal decrease in the pituitary stalk when compared to that in the anterior pituitary gland. Satogami et al. [17] mentioned that the peripheral rim on T2-weighted imaging might correspond to the pars tuberalis in the pituitary stalk. We used relatively high-resolution imaging for T1WI; however, such zonal anatomy of the pituitary stalk was not seen in this study. Other possible causes for the high signal intensity in the pituitary stalk include developing portal vessels and clock gene proteins, which were previously studied in beagles [26] and mice [27]. However, these structures do not decrease in size following birth and seem unlikely to be a cause of high signal in the pituitary stalk.

Thin-slice T1WI demonstrated various signal intensities of the pituitary stalk. A normal pituitary stalk shows low-to-intermediate signal intensity when compared to that of white matter on T1WI in adults, but assessment in infants is sometimes difficult. We set thin-slice T1WI to be performed in a relatively short time. Technical factors, such as partial volume effect and slight motion artifact, might reduce the signal intensity of the pituitary stalk. MR imaging for a high resolution and high signal-to-noise ratio usually requires a long scan time. However, a long scan time may induce a change to contain motion artifact. Recent techniques, such as the motion correction method, parallel imaging for 3D imaging, and compressed sensing [28–30], may improve pituitary stalk visibility in infants.

The present study had several limitations. First, some infants were excluded because of severe motion artifacts. Even after excluding these infants, a small amount of motion might have affected the visibility and signal intensity of the pituitary stalk in some selected infants. Although we used immobilization and a relatively short scan time during natural sleep [31], motion could not be completely avoided. Nevertheless, most of the infants successfully underwent thin-slice T1WI, and the success rate for MR imaging in this study was comparable or slightly lower than that for body MR imaging without sedation in a previous report [32]. Second, we could not compare MR findings with histological findings. As the included infants were considered to be normal or near normal, histological assessments could not be performed. Third, as the included infants were scanned

mainly for screening, minor clinical insults might have affected the status of the pituitary stalk. Moreover, some effect of premature delivery on the signal increase in the pituitary stalk could not be denied. Further assessments are needed. Fourth, serial MR examinations were not performed. Therefore, individual serial changes in the signal intensity of the pituitary stalk were not assessed in this study. Fifth, the two MR scanners used in this study might have some differences in signal-to-noise ratio. Generally, multichannel surface coils increase surface signal gain, whereas the signal gain decreases depending on the distance from the coils [33,34]. To correct this, normalization of signal-intensity inhomogeneity technique (CLEAR, Philips, The Netherlands) were used in this study. We believe that the central signal drop was corrected to some extent between the two scanners. In addition, we assessed the signal intensity of the pituitary stalk normalized by that of the pons. However, the image quality might have been slightly different between the scanners.

In conclusion, our study showed that there is a negative correlation between the signal intensity of the pituitary stalk on T1WI and CA. This might be related to postnatal changes in the pars tuberalis of the pituitary stalk.

## Appendix A. Supplementary material

Supplementary data to this article can be found online at <https://doi.org/10.1016/j.braindev.2018.11.009>.

## References

- [1] Plaisier A, Govaert P, Lequin MH, Dudink J. Optimal timing of cerebral MRI in preterm infants to predict long-term neurodevelopmental outcome: a systematic review. *AJNR Am J Neuroradiol* 2014;35:841–7.
- [2] Argyropoulou MI. Brain lesions in preterm infants: initial diagnosis and follow-up. *Pediatr Radiol* 2010;40:811–8.
- [3] Branson HM. Normal myelination: a practical pictorial review. *Neuroimaging Clin N Am* 2013;23:183–95.
- [4] Barkovich AJ. Magnetic resonance techniques in the assessment of myelin and myelination. *J Inher Metab Dis* 2005;28:311–43.
- [5] Engle WA, American Academy of pediatrics committee on F, newborn. Age terminology during the perinatal period. *Pediatrics* 2004;114:1362–4.
- [6] van de Bor M, Guit GL, Schreuder AM, van Bel F, Wondergem J, den Ouden L, et al. Does very preterm birth impair myelination of the central nervous system? *Neuropediatrics* 1990;21:37–9.
- [7] Konishi Y, Hayakawa K, Kuriyama M, Fujii Y, Sudo M, Konishi K, et al. Developmental features of the brain in preterm and fullterm infants on MR imaging. *Early Hum Dev* 1993;34:155–62.
- [8] Kitamura E, Miki Y, Kawai M, Itoh H, Yura S, Mori N, et al. T1 signal intensity and height of the anterior pituitary in neonates: correlation with postnatal time. *AJNR Am J Neuroradiol* 2008;29:1257–60.
- [9] Taoka T, Aida N, Ochi T, Takahashi Y, Akashi T, Miyasaka T, et al. Transient hyperintensity in the subthalamic nucleus and

- globus pallidus of newborns on T1-weighted images. *AJNR Am J Neuroradiol* 2011;32:1130–7.
- [10] Hori S, Taoka T, Ochi T, Miyasaka T, Sakamoto M, Takayama K, et al. Structures showing negative correlations of signal intensity with postnatal age on T1-weighted imaging of the brain of newborns and infants. *Magn Reson Med* 2017;16:325–31.
- [11] Arthur R. Magnetic resonance imaging in preterm infants. *Pediatr Radiol* 2006;36:593–607.
- [12] Beitzke D, Simbrunner J, Riccabona M. MRI in paediatric hypoxic-ischemic disease, metabolic disorders and malformations—a review. *Eur J Radiol* 2008;68:199–213.
- [13] Valkama AM, Paakko EL, Vainionpaa LK, Lanning FP, Ilkko EA, Koivisto ME. Magnetic resonance imaging at term and neuromotor outcome in preterm infants. *Acta Paediatr* 2000;89:348–55.
- [14] Arthurs OJ, Edwards A, Austin T, Graves MJ, Lomas DJ. The challenges of neonatal magnetic resonance imaging. *Pediatr Radiol* 2012;42:1183–94.
- [15] Tyan AE, McKinney AM, Hanson TJ, Truwit CL. Comparison of spin-echo and gradient-echo T1-weighted and spin-echo T2-weighted images at 3T in evaluating term-neonatal myelination. *AJNR Am J Neuroradiol* 2015;36:411–6.
- [16] Landis JR, Koch GG. The measurement of observer agreement for categorical data. *Biometrics* 1977;33:159–74.
- [17] Satogami N, Miki Y, Koyama T, Kataoka M, Togashi K. Normal pituitary stalk: high-resolution MR imaging at 3T. *AJNR Am J Neuroradiol* 2010;31:355–9.
- [18] Hamilton BE, Salzman KL, Osborn AG. Anatomic and pathologic spectrum of pituitary infundibulum lesions. *AJR Am J Roentgenol* 2007;188:W223–32.
- [19] Cox TD, Elster AD. Normal pituitary gland: changes in shape, size, and signal intensity during the 1st year of life at MR imaging. *Radiology* 1991;179:721–4.
- [20] Wolpert SM, Osborne M, Anderson M, Runge VM. The bright pituitary gland—a normal MR appearance in infancy. *AJNR Am J Neuroradiol* 1988;9:1–3.
- [21] Younes MA, Besch NF, Besch PK. Estradiol and progesterone binding in human term placental cytosol. *Am J Obstet Gynecol* 1981;141:170–4.
- [22] Sarda IR, Gorwill RH. Hormonal studies in pregnancy: I. Total unconjugated estrogens in maternal peripheral vein, cord vein, and cord artery serum at delivery. *Am J Obstet Gynecol* 1976;124:234–8.
- [23] Kelberman D, Dattani MT. Hypothalamic and pituitary development: novel insights into the aetiology. *Eur J Endocrinol* 2007;157(Suppl 1):S3–S14.
- [24] Lu YT, Qi ST, Xu JM, Pan J, Shi J. A membranous structure separating the adenohypophysis and neurohypophysis: an anatomical study and its clinical application for craniopharyngioma. *J Neurosurg Pediatr* 2015;15:630–7.
- [25] Rudolf T, Filler T, Wittkowski W. Pars tuberalis specific cells within the pars distalis of the adenohypophysis. An ontogenetic study. *Ann Anat* 1993;175:171–6.
- [26] Sasaki F, Nishioka S. Fetal development of the pituitary gland in the beagle. *Anat Rec* 1998;251:143–51.
- [27] Ansari N, Agathagelidis M, Lee C, Korf HW, von Gall C. Differential maturation of circadian rhythms in clock gene proteins in the suprachiasmatic nucleus and the pars tuberalis during mouse ontogeny. *Eur J Neurosci* 2009;29:477–89.
- [28] Lv J, Yang M, Zhang J, Wang X. Respiratory motion correction for free-breathing 3D abdominal MRI using CNN-based image registration: a feasibility study. *Br J Radiol* 2018;91:20170788.
- [29] Jaimes C, Gee MS. Strategies to minimize sedation in pediatric body magnetic resonance imaging. *Pediatr Radiol* 2016;46:916–27.
- [30] Runge VM, Richter JK, Heverhagen JT. Speed in clinical magnetic resonance. *Invest Radiol* 2017;52:1–17.
- [31] Parad RB. Non-sedation of the neonate for radiologic procedures. *Pediatr Radiol* 2018;48:524–30.
- [32] Gale C, Jeffries S, Logan KM, Chappell KE, Uthaya SN, Modi N. Avoiding sedation in research MRI and spectroscopy in infants: our approach, success rate and prevalence of incidental findings. *Arch Dis Child Fetal Neonatal Ed* 2013;98:F267–8.
- [33] Parikh PT, Sandhu GS, Blackham KA, Coffey MD, Hsu D, Liu K, et al. Evaluation of image quality of a 32-channel versus a 12-channel head coil at 1.5T for MR imaging of the brain. *AJNR Am J Neuroradiol* 2011;32:365–73.
- [34] Wang J, Qiu M, Constable RT. In vivo method for correcting transmit/receive nonuniformities with phased array coils. *Magn Reson Med* 2005;53:666–74.